Immunopathology and Infectious Diseases

Association of T-Zone Reticular Networks and Conduits with Ectopic Lymphoid Tissues in Mice and Humans

Alexander Link,* Debbie L. Hardie,[†]
Stéphanie Favre,* Mirjam R. Britschgi,*
David H. Adams,[†] Michael Sixt,[‡]
Jason G. Cyster,[§] Christopher D. Buckley,[†]
and Sanjiv A. Luther*

From the Department of Biochemistry, University of Lausanne, Epalinges, Switzerland; the School of Immunity and Infection,[†] Institute for Biomedical Research, Medical Research Council Center for Immune Regulation, University of Birmingham, Birmingham, United Kingdom; the Department of Molecular Medicine,[‡] Max Planck Institute of Biochemistry, Martinsried, Germany; and the Howard Hughes Medical Institute and Department of Microbiology and Immunology,[§] University of California San Francisco, San Francisco, California*

Ectopic or tertiary lymphoid tissues (TLTs) are often induced at sites of chronic inflammation. They typically contain various hematopoietic cell types, high endothelial venules, and follicular dendritic cells; and are organized in lymph node–like structures. Although fibroblastic stromal cells may play a role in TLT induction and persistence, they have remained poorly defined. Herein, we report that TLTs arising during inflammation in mice and humans in a variety of tissues (eg, pancreas, kidney, liver, and salivary gland) contain stromal cell networks consisting of podoplanin+ T-zone fibroblastic reticular cells (TRCs), distinct from follicular dendritic cells. Similar to lymph nodes, TRCs were present throughout T-cell–rich areas and had dendritic cells associated with them. They expressed lymphotoxin (LT) β receptor (LTβR), produced CCL21, and formed a functional conduit system. In rat insulin promoter–CXCL13–transgenic pancreas, the maintenance of TRC networks and conduits was partially dependent on LTβR and on lymphoid tissue inducer cells expressing LTβR ligands. In conclusion, TRCs and conduits are hallmarks of secondary lymphoid organs and of well-developed TLTs, in both mice and humans, and are likely to act as important scaffold and organizer cells of the T-cell–rich zone. *(Am J Pathol 2011, 178:1662–1675; DOI: 10.1016/j.ajpath.2010.12.039)*

Acute inflammation has evolved to facilitate effective elimination of pathogens and tumors. It is normally transient and turned off when the causative stimulus has been eliminated. Occasionally, the inflammation is sustained and becomes persistent.[1] This complex pathophysiological process is characterized by the infiltration of target organs, with lymphocytes organizing themselves into distinct T- and B-cell–rich zones. Because these infiltrates show considerable morphological, cellular, and molecular similarities to secondary lymphoid organs (SLOs), especially lymph nodes (LNs), they are referred to as tertiary lymphoid tissues (TLTs). There is increasing evidence that these TLTs, observed within a wide range of inflamed tissues, are immunologically active and have the potential to cause severe tissue damage.[2–4]

Specialized stromal cell types present within inflamed tissues are thought to be critical for the switch from acute to chronic inflammation and for disease persistence.[1] In particular, high endothelial venules (HEVs), follicular dendritic cells (FDCs), and fibroblasts are hallmarks of many TLT types.[2,3] However, the presence and role of T-zone fibro-

blastic reticular cells (TRCs or T-FRC) in the formation and persistence of TLTs has not yet been carefully examined. In murine SLOs, FDCs and TRCs form a dense three-dimensional (3D) network throughout the B and T zones, respectively.[5–7] The TRCs serve as a scaffold for lymphocyte migration within the T zone.[8] They produce the CCR7 ligands, CCL19 and CCL21, required for T-cell attraction and motility and dendritic cell attraction.[9–11] They also regulate the survival of naïve T cells by producing IL-7.[10] Finally, they produce the extracellular matrix (ECM) scaffold that forms a network of microvessels, called conduits.[7,12,13] In LNs, these conduits drain fluid and small molecules from the subcapsular sinus to HEVs.[13,14] Thus far, no single marker unambiguously identifies TRCs in murine SLOs. The TRCs can be identified by their T-zone localization, reticular morphological features, and surface expression of podoplanin (also referred to as gp38); and the absence of endothelial (CD31 or LYVE-1), FDC (CD21/35), and hematopoietic (CD45) markers.[6,10,12] In humans, podoplanin has been widely used as a marker for lymphatic endothelial cells[15]; recently, it was used for the identification of FDC[16,17] and cancer-associated fibroblasts.[18,19]

Reticular networks of podoplanin$^+$ and BP-3$^+$ stromal cells have also been observed in murine TLTs, such as pancreatic infiltrates of rat insulin promoter (RIP)–CCL19, RIP-CCL21, and RIP-CXCL13 animals,[20,21] and recently at sites of acute inflammation and tumors.[22] By using the antibody ER-TR7, similar networks have been visualized in other murine inflammation models.[20,23–25] However, recent evidence[10,12,13] suggests that ER-TR7 stains a conduit component, rather than TRCs. In human tissues, such as LNs and arthritic joints, the presence of reticular cells in the T zone expressing α smooth muscle actin (αSMA), CCL19, and CCL21 has recently been reported.[26] However, a detailed characterization of stromal cells of the T zone has been lacking for murine TLTs and human SLOs and TLTs.

The formation of TLTs in adult mice is thought to be governed by the same factors that regulate LN and Peyer's patch (PP) development during embryonic and postnatal life.[2,3] Members of the tumor necrosis factor–lymphotoxin (LT) family and lymphoid tissue chemokines (ie, CXCL13, CCL19, and CCL21) are central to this process. Lymphoid tissue inducer (LTi) cells express cell surface LT$\alpha\beta$ and trigger the LTβ receptor (LTβR) present on fibroblastic stromal cells, thereby starting extensive hematopoietic-stromal cell cross talk.[27,28] This induces the expression of CCL19, CCL21, and CXCL13 and adhesion molecules by these stromal cells. The chemokines then attract more LTi cells expressing the chemokine receptors CCR7 and CXCR5 that bind the ligands CCL19/CCL21 and CXCL13, respectively. Finally, the development of HEVs brings in many more lymphocytes, leading to large T- and B-cell compartments. Consistent with this model, the expression of LTα, LT$\alpha\beta$, tumor necrosis factor-α, CXCL13, CCL19, or CCL21 under the RIP induces the formation of extensive TLT structures next to pancreatic islets.[2,3,20,21,29–32] The observation that TLT structures require LT$\alpha\beta$ signaling for their induction and maintenance suggested that they also depend on cross talk between LT$\alpha\beta^+$ hematopoietic cells and LTβR$^+$ stromal cells.[33] The LT$\alpha\beta^+$ LTi cells have been shown to be present in adult spleen.[34–36] The observation of LTi-like cells in pancreatic islets of neonatal RIP-CXCL13 mice[37] suggested that they may play a role in TLT development. The role of LTi cells in this process is controversial,[25,38] as is the identity of the LTβR-expressing stromal cells.[4,28]

Herein, we performed a detailed characterization of stromal cell subsets in murine and human TLTs and in human SLOs. We provide several lines of evidence suggesting that TRC-like cells exist in human SLOs and in infiltrates of two chronic immune-mediated inflammatory diseases in humans [ie, primary biliary cirrhosis (PBC)[39] and Sjögren's syndrome].[40] Similar TRC networks were associated with the T-cell–rich infiltrate of several murine models of chronic inflammation.[21,30] Their phenotype closely resembled their counterpart in SLOs. We further dissected the cells and signals required for RIP-CXCL13–driven formation of ectopic TRCs and provide evidence that their maintenance is dependent on LT$\alpha\beta$-expressing LTi cells.

Materials and Methods

Mice

The following mouse strains were used (aged 3 to 6 months): C57BL/6 (B6; Janvier, Le Chenest-Saint-Isle, France) RIP-LTα[29] (provided by Mathias Heikenwälder, University Hospital Zurich, Zurich, Switzerland; originally from Nancy Ruddle, Yale University, New Haven, CT), non-obese diabetic (NOD) (Jackson, Bar Harbor, ME), RIP-CXCL13,[21] retinoid-related orphan receptor (ROR)$\gamma^{-/-}$,[41] (provided by Dan Littman, New York University, New York), and T cell receptor (TCR) $\beta\delta^{-/-}$ (Jackson). Some adult (aged 4 months) RIP-CXCL13–transgenic animals were injected i.p. twice per week for 22 days with 100 μg of soluble murine LTβR or control human LFA3 (CD58) fused to the Fc portion of human IgG1, as previously described[42] (provided by Jeff Browning, Biogen Idec, Boston, MA). All mice were maintained under pathogen-free conditions. All mouse experiments were authorized by the Swiss Federal Veterinary Office.

Human Tissue Samples

Tonsils ($n = 5$) were removed from patients undergoing routine tonsillectomy, and mesenteric LNs ($n = 1$) and livers were removed from patients during liver transplantation (normal liver, $n = 1$; PBC liver, $n = 4$; two contained well-defined TLT structures at several levels). Sjögren's syndrome salivary gland tissue ($n = 10$; two contained well-defined TLT structures at several levels) was obtained for biopsy. All human tissue samples were frozen in liquid nitrogen. Ethical approval for the use of tissue samples taken during this study was obtained from the Birmingham and local Research Ethics Committee (REC 2002/088, LREC 5735, and 06/Q2706/66).

Table 1. List of the Staining Reagents Used

Target	Species	Clone or designation	Conjugate	Supplier and catalog number
Primary antibodies for immunofluorescence staining of human tissue sections				
Podoplanin	Mouse IgG1	4D5aE5E6 (MCA 2370)	Purified	AbD Serotec
Podoplanin	Mouse IgG1	D2-40 (730-01)	Purified	Signet
CD3	Mouse IgG2b	UCHT-1	Purified	Peter Beverley (UCL)
CD21	Mouse IgG2a	HB5	Purified	Thomas Tedder (Duke University)
CCL21	Rabbit IgG1		Purified	Abcam ab9851
Podoplanin	Rabbit		Purified	Abcam ab10274
CD11c	Mouse IgG1	BU15	Purified	Hybridoma
Collagen-1	Goat		Purified	Southern Biotechnologies (SB) 01310-01
Laminin	Rabbit		Purified	Sigma L9393
CD31	Mouse IgG2a	HEC7 (MA3100)	Purified	Thermo Scientific
Lyve-1	Mouse IgG1	8C	Purified	David Jackson (Oxford)
Secondary antibodies for immunofluorescence staining of human tissue sections				
Anti-mouse IgG1	Goat		FITC	SB 1070-02
Anti-fluorescein	Goat		Alexa488	Invitrogen A11096
Anti-mouse IgG2b	Goat		Cy5	SB 1090-15
Anti-mouse IgG2a	Goat		Alexa350	Invitrogen A21130
Anti-rabbit IgG	Donkey		TRITC	Jackson ImmunoResearch 711-026-152
Anti-mouse IgG	Donkey		Cy5	Jackson ImmunoResearch 715-176-151
Anti-goat IgG	Donkey		FITC	Jackson ImmunoResearch 705-096-147
Primary antibodies for immunofluorescence staining of murine tissue sections				
B220	Rat	RA3-6B2	Purified	Hybridoma
BP-3 (CD157)	Mouse	BP-3	Biotin	Max D. Cooper (Birmingham, Alabama)
CCL21	Goat	AF457	Purified	R&D Systems
CD35 (CR1)	Rat	8C12	Purified	Hybridoma
CD3ε	Armenian hamster	145-2C11	Purified	Hybridoma
CD4	Rat	H129.19.6	Purified	Biolegend
Desmin	Rabbit	No. 10570	Purified	PROGEN
ER-TR7	Rat	ER-TR7	Purified	Willem van Ewijk (Leiden, the Netherlands)
Podoplanin (gp38)	Syrian hamster	8.1.1	Purified	Developmental Studies Hybridoma Bank
PECAM-1 (CD31)	Rat	GC-51	Purified	Beat Imhof (Geneva, Switzerland)
CD11c	Armenian hamster	N418	Biotin	eBioscience
VCAM-1 (CD106)	Rat	M/K2.7	Biotin	Hybridoma, ATCC
LTβR	Rat	4H8 WH2	Purified	Axxora Corporation
MAdCAM-1	Rat	Meca-89	Biotin	Hybridoma, ATCC
PDGFRα (CD140a)	Rat	APA5	Purified	eBioscience
PDGFRβ (CD140b)	Rat	APB5	Purified	eBioscience
CCL21	Goat	AF457	Purified	R&D Systems
Laminin	Rabbit	L9393	Purified	Sigma
Collagen-1	Goat	1310-01	Purified	Southern Biotech
Fibronectin	Rabbit	F3648	Purified	Sigma
Lyve-1	Rabbit	103-PA50	Purified	Reliatech
MHC II (I-A/I-E)	Rat	2G9	Purified	BD Biosciences
PNAd	Rat	MECA-79	Purified	BD Biosciences
Insulin	Guinea pig	4012-01	Purified	Linco Research
Secondary reagents for immunofluorescence staining of murine tissue sections				
Anti-Syrian hamster IgG	Goat	Polyclonal	Cy3	Jackson ImmunoResearch
Anti-Syrian hamster IgG	Goat	Polyclonal	Biotin	Jackson ImmunoResearch
Anti-Syrian hamster IgG	Goat	Polyclonal	Cy3	Jackson ImmunoResearch

(table continues)

Table 1. *Continued*

Target	Species	Clone or designation	Conjugate	Supplier and catalog number
Anti-Armenian hamster IgG	Goat	Polyclonal	Biotin	Jackson ImmunoResearch
Anti-guinea pig	Goat	Polyclonal	Biotin	Vector
Anti-rat IgG	Donkey	Polyclonal	APC	Jackson ImmunoResearch
Anti-rat IgG	Donkey	Polyclonal	Alexa488	Molecular Probes
Anti-goat IgG	Donkey	Polyclonal	Biotin	Jackson ImmunoResearch
Anti-rabbit IgG	Donkey	Polyclonal	Alexa488	Molecular Probes
Anti-rabbit IgG	Donkey	Polyclonal	Cy3	Jackson ImmunoResearch
Streptavidin			APC	Biolegend
Streptavidin			Alexa488	Molecular Probes
Streptavidin			Cy3	Jackson ImmunoResearch
Primary reagents for flow cytometric analysis of murine cells				
IL-7Rα (CD127)	Rat	A7R34	PE	eBioscience
CD4	Rat	GK1.5	APC	BioLegend
CD3ε	Armenian hamster	145-2C11	FITC	BioLegend
CD11c	Armenian hamster	N418	FITC	eBioscience
CD19	Rat	6D5	FITC	BioLegend
CD45	Rat	30-F11	PE-Cy7	BioLegend
Secondary reagents for flow cytometric analysis of murine cells				
Streptavidin		12-4317-87	PE	eBioscience
Streptavidin		35-4317-82	PE-Cy5	eBioscience
Anti-human IgG	Goat	109-066-098	Biotin	Jackson ImmunoResearch
Anti-rat IgG (H+L)	Donkey	712-116-153	PE	Jackson ImmunoResearch

APC, allophycocyanin; FITC, fluorescein isothiocyanate; MHC, major histocompatibility complex; PE, phycoerythrin; PECAM, platelet endothelial cell adhesion molecule; TRITC, tetramethylrhodamine isothiocyanate; VCAM, vascular cell adhesion molecule; MAdCAM, mucosal addressin cell adhesion molecule; PDGFR, platelet derived growth factor receptor; PNAd, peripheral lymph node addressin.

Immunofluorescence Microscopy on Human Tissue Samples

Acetone-fixed 5-μm sections of snap-frozen tissues were prepared and stained, as previously described,[43] with the antibodies listed in Table 1. Slides were mounted in 2.4% w/v 1,4-diazabicyclo(2,2,2)octane (Aldrich, Gillingham, England) in 10% v/v glycerol (Fisons Scientific, Loughborough, UK) in PBS (pH, 8.6) and analyzed by confocal microscopy (LSM 510; Carl Zeiss Ltd, Welwyn Garden City, England).

Immunofluorescence Microscopy on Murine Tissues

To visualize functional conduits, Texas Red–labeled 10-kDa dextran (Invitrogen AG, Basel, Switzerland) was injected i.v. and mice were sacrificed 5 minutes later. The pancreas was removed, fixed in four percent paraformaldehyde at 4°C, and saturated in 30% sucrose for 3 hours at 4°C before embedding in Optimal Cutting Compound (OCT, Tissue-Tek; Sakura), followed by freezing in an ethanol dry ice bath. For all other experiments, dissected tissues were embedded in OCT without prior fixation. Immunofluorescence stainings were performed on cryostat sections (8 μm) with the antibodies listed in Table 1, as previously described.[10] For podoplanin and CCL21, primary antibodies were revealed using biotinylated secondary antibodies and streptavidin–horseradish peroxidase, followed by tyramide signal amplification (kit 22; Invitrogen), according to the manufacturer's instructions; however, a borate

buffer (0.1 mol/L in PBS, pH 8.5) was used for tyramide dilution. Images were acquired on a microscope (Axioplan) with AxioCam MRm (Zeiss) or on a different microscope (DM IRE2) with laser-scanning confocal head TCS SP2 AOBS (acoustic optical beam splitter; Leica, Nunningen, Switzerland).

Vibratome Sections and Immunofluorescence Staining

Isolated peripheral LNs and pancreas were fixed overnight at 4°C in freshly prepared one percent paraformaldehyde (in PBS), washed, and embedded in four percent low-gelling agarose (Sigma) in PBS; 100- to 200-μm sections were cut using a vibratome (Microm HM 650V). Sections were blocked with one percent bovine serum albumin for 1 hour and stained for at least 3 hours or overnight with the antibodies listed in Table 1. Subsequently, sections were washed extensively in PBS and embedded using Mowiol 4-88 (Merck, Darmstadt, Germany). Images were taken with an upright microscope (Axio Imager with ApoTome; Zeiss). The 3D image reconstructions were made with Axio Vision software version 4.8.1 (Zeiss).

Isolation of LTi Cells

Peripheral LNs, spleen, or pancreas was dissected from euthanized mice. The capsule of the LNs was opened with 26-gauge syringe needles; the spleen and pancreas were cut into small pieces. The LN, spleen, and pancreas pieces were then digested with gentle stirring for 20 minutes at

37°C in 2 mL of RPMI 1640 medium containing 1 mg/mL collagenase IV (Worthington, Lakewood, NJ), 40 μg/mL DNase I (Roche, Basel, Switzerland), and two percent (v/v) FBS. Collagenase D, 1 mg/mL (Roche), was added; and digestion continued for another 20 minutes. Every 10 minutes, the suspension was gently pipetted to break up remaining aggregates until no visible fragments remained. During the last pipetting, EDTA was added to a final concentration of 5 mmol/L to further reduce cell aggregates. Cells were then passed through a 40-μm mesh, washed twice, and resuspended in RPMI 1640 medium containing two percent (v/v) FBS and 5 μg/mL DNase I at a maximum concentration of 2×10^7 cells/mL. The cell suspension was then underlayed with 2.5 mL of mixed Lympholyte M (Cedarlane, Burlington, VT) at 25°C and centrifuged at $750 \times g$ for 20 minutes. The cells at the gradient interphase were collected and used for flow cytometry.

Flow Cytometry

Stainings were performed with 1×10^5 to 1.5×10^6 cells in 96-well V-bottom plates (Falcon; Milian AG, Geneva, Switzerland). Cells were blocked with one percent normal mouse serum and stained with the antibodies listed in Table 1 in 25 μL of PBS containing two percent FBS, 2 mmol/L EDTA, and 0.1% NaN$_3$; the cells were washed twice with 200 μL of this buffer after each step. Uncojugated primary antibodies were detected with the secondary reagents listed in Table 1. Data were acquired on a flow cytometer (FACSCanto; BD Biosciences, Basel, Switzerland) and analyzed with Flowjo software version 9.1 (TreeStar, Ashland, OR). To detect surface expression of LTβR, cells were pretreated with FcR blocking antibody (2.4.G2; BD Biosciences) and 0.5% normal mouse and rat serum. The LTβR-Fc (provided by J. Browning) and the FN14-Fc (provided by P. Schneider) (both human IgG1) were added and detected using a biotinylated goat anti-human IgG (Jackson ImmunoResearch, Newmarket, UK) pretreated for 30 minutes with four percent normal mouse and rat serum. Finally, streptavidin-phycoerythrin (eBioscience, San Diego, CA) was added, along with other surface markers.

In Situ *Hybridization*

Mice were anesthetized and perfused with PBS, followed by four percent paraformaldehyde in PBS. The pancreas was then removed and further fixed in four percent paraformaldehyde overnight and saturated in 30% sucrose for 3 hours at 4°C before embedding in OCT, followed by freezing in an ethanol–dry ice bath. Frozen sections (8 μm) were then treated as previously described[9] and hybridized overnight at 60°C with a CCL21-antisense digoxigenin-labeled riboprobe in hybridization solution. After washing at high stringency, sections were incubated with sheep anti-digoxigenin (Roche), followed by alkaline phosphatase–coupled donkey anti-sheep antibody (Jackson ImmunoResearch Laboratories) and developed with Nitroblue-tetrazolium-chloride (NBT, Bio-Rad) and 5-Bromo-4-chloro-3-indolyl phospate (BCIP, Sigma).

Statistical Analysis

Statistical significance was determined using an unpaired two-tailed Student's *t*-test. A Levene's test for homogeneity of variances was used to check for equal variance. An unpaired two-tailed Student's *t*-test for unequal variance was used. $P < 0.05$ indicated significance.

Results

Podoplanin Identifies T-Zone Reticular Networks in Human Secondary Tissues and TLTs

To determine whether human SLOs and TLTs develop a TRC network similar to murine SLOs,[10,12] we analyzed histological sections for the presence of podoplanin$^+$ reticular cells. Three different antibodies to podoplanin comparably labeled the reticular networks of the T zone in both human LNs and tonsils (Figure 1, see Supplemental Figure S1 at *http://ajp.amjpathol.org*), while labeling most strongly FDCs and lymphatic vessels. The podoplanin$^+$ cells of the T zone could be distinguished from FDCs through their localization among T cells and the absence of CD21 (Figure 1) and from lymphatic vessels by their reticular morphological features and absence of the endothelial marker CD31 and the lymphatic marker Lyve-1 (see Supplemental Figure S2 at *http://ajp.amjpathol.org*). Ectopic lymphoid infiltrates occurring in chronically inflamed nonlymphoid tissues, such as PBC liver or Sjögren's syndrome salivary gland, showed similar reticular networks of podoplanin$^+$ CD31$^-$Lyve1$^-$ cells in some, but not all, CD3$^+$ T-cell areas (Figure 1, see Supplemental Figures S2 and S3 at *http://ajp.amjpathol. org*). Similar to LNs and tonsils, podoplanin- and CD21-coexpressing FDCs were observed as dense clusters inside B-cell rich zones. However, in noninflamed liver, podoplanin-expressing cells were virtually absent. These results suggest that TRC-like cells are present in human SLOs and can develop at sites of chronic inflammation.

Podoplanin$^+$ Stromal Cells in Human Tissues Share Many Properties with Murine TRCs

To test whether these TRC-like cells observed in human tissues share other properties with TRCs characterized in murine LNs and spleen, we further defined these cells histologically. In T zones of LNs and tonsils, podoplanin$^+$ cells formed a dense reticular network that associated with ECM molecules (ie, collagen-1, laminin, and fibronectin) (Figure 2, data not shown) in structures that resemble, in their composition and morphological features, the conduits found in murine SLOs.[13] Podoplanin$^+$ cells colocalized with CCL21 protein and were in close contact with CD11c-positive dendritic cells (Figure 2). Similarly, at sites of chronic inflammation, such as PBC liver and Sjögren's syndrome salivary gland, but not in healthy liver, ECM fibers were observed in association with podoplanin$^+$ cells in T cell–rich infiltrates (Figure 2). To a variable extent, TRC-like cells displayed some detectable CCL21 protein and were associated with DCs. Together, these data indicate a high similarity of the

higher magnification of T zone

| Podoplanin | CD21 | CD3 | merge | Podoplanin | merge |
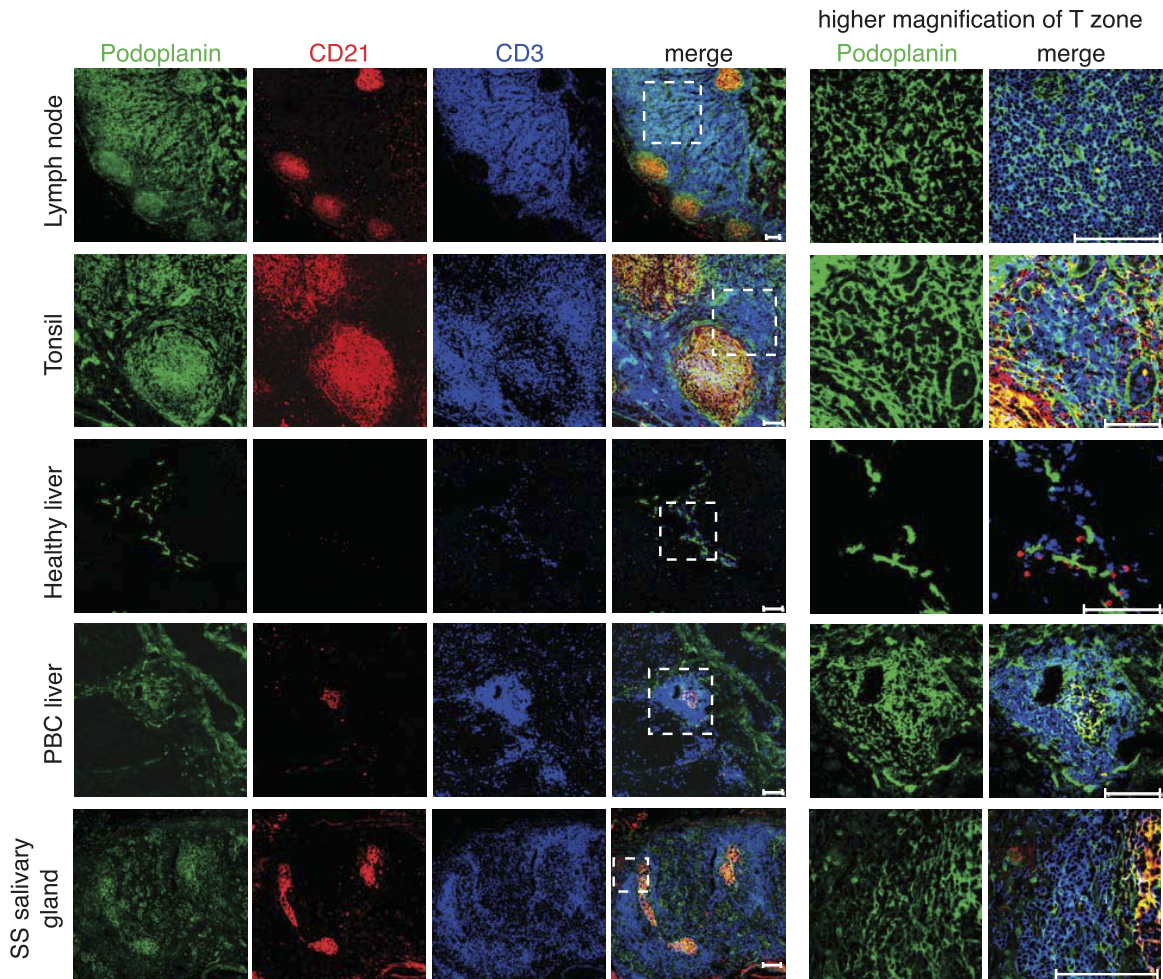
Figure 1. Podoplanin^{+} CD21^{−} reticular cell networks are associated with CD3^{+} T-cell areas in human LNs and TLTs. Immunofluorescence analysis of human SLOs, such as LNs and tonsils, and TLTs, such as inflamed PBC liver (*n* = 2) and inflamed salivary gland from a patient with Sjögren's syndrome (SS) (*n* = 2). Healthy liver that expressed little podoplanin served as a control. Podoplanin^{+} cells are shown in green; CD21^{+} FDC, red; and CD3^{+} T cells, blue. A higher magnification of the T-cell–rich zone is shown in the two **right columns**. Scale bars = 100 μm.

stromal compartments of the T zone between murine SLOs and human lymphoid tissues.

Podoplanin[+] Stromal Cells Are Present in Murine TLTs

To study the development and properties of TLT-associated TRCs in greater detail, we tested several mouse models displaying lymphocytic tissue infiltration for the presence of these stromal cells: NOD mice that are a model of autoimmune diabetes mellitus and develop mostly smaller pancreatic lymphoid infiltrates[44] and RIP-LTα transgenic and RIP-CXCL13 mice that form large infiltrates of mostly naïve T and B cells in kidney and pancreas, respectively, without causing overt disease.[21,29,30] Similar to murine LNs, reticular podoplanin[+] cell networks were present in the T- but not the B-cell–rich areas in TLTs of all three mouse models. These fibroblastic cells showed a surface phenotype distinct from podoplanin^{−} CD31^{high} blood vessels and podoplanin^{+/−} lyve1^{+} lymphatic vessels associated with the infiltrate, in addition to their difference in cell morphological features and organization (Figure 3, A and B; see Supplemental

Figure S4 at *http://ajp.amjpathol.org*). Although large and intermediate infiltrates with well-developed T-cell areas were always associated with a reticular podoplanin[+] cell network, smaller infiltrates without a T zone were often lacking it (not shown). A higher magnification showed that the podoplanin^{+} stromal cells also expressed desmin and surrounded conduit-like structures recognized by the ER-TR7 antibody, similar to LNs (Figure 3C). Contrary to a previous report,[21] we occasionally found CD35^{+} FDCs inside the B-cell follicles of large RIP-CXCL13 infiltrates. However, the podoplanin^{+} cell network in the T zone was always CD35^{−} (Figure 3D), suggesting the presence of two distinct stromal cell networks. Therefore, TLTs in all three tissue infiltration models displayed reticular podoplanin[+] cell networks with a close resemblance to the TRC network of the LN T zone.

### T-Zone Reticular Networks Share Phenotypic and Functional Features with LN TRCs

To further compare the phenotype of podoplanin^{+} CD31^{−} stromal cells found in TLTs with their counterparts in
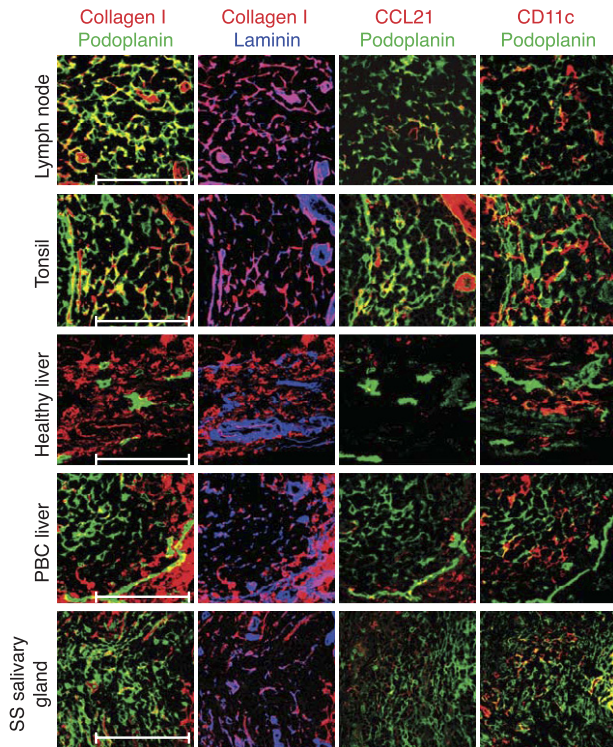
Figure 2. The podoplanin$^+$ CD21$^-$ cell network in human tissues is associated with ECM fibers, the chemokine CCL21 and CD11c$^+$ dendritic cells. Immunofluorescence analysis of human SLOs, such as LNs and tonsils; and TLTs, such as inflamed PBC liver and inflamed salivary gland [Sjögren's syndrome (SS)]. Healthy liver served as a control. Podoplanin (green), collagen-1 (red), laminin (blue), CCL21 (red), and CD11c (red) in CD3$^+$ T-cell areas are shown. Scale bars = 100 μm.

LNs,[10,12] a panel of markers was tested on pancreatic infiltrates of RIP-CXCL13–transgenic mice, which, among the three mouse models, displayed the highest frequency of large infiltrates and lymphoid tissue structures. Confocal microscopic images showed that many TRC markers, including BP-3, vascular cell adhesion molecule-1 (VCAM-1), platelet-derived growth factor receptor (PDGFR)α/β, and LTβR, colocalized with podoplanin staining (Figure 4A). Comparable to LNs,[10] most CCL21 protein was localized in conduit-like structures that were enwrapped by podoplanin$^+$ stromal cells (Figure 4B). By using *in situ* hybridization analysis, we detected *Ccl21* mRNA expression on HEVs and in a reticular pattern in the T-cell–rich zone of pancreatic infiltrates, indicating that the CCL21 protein is locally produced (Figure 4C). To determine whether TLTs also form a conduit system, as found in SLOs,[13,14] ectopic pancreatic infiltrates of RIP-CXCL13 transgenic (tg) mice were labeled with antibodies to podoplanin and various ECM molecules. A 3D reconstruction of confocal microscopic images, obtained from thick vibratome sections, confirmed that TLTs develop 3D networks of podoplanin$^+$ cells wrapping around laminin$^+$ matrix structures, similar to LNs (Figure 4D). These structures consisted of a cellular layer expressing podoplanin, a basement membrane containing fibronectin and laminin, and a core containing collagen-1 (Figure 4E). Pancreatic infiltrates in prediabetic NOD mice displayed matrix structures with the same composition (Figure 4E). The functionality of the conduits present in RIP-

CXCL13 tg$^+$ pancreata was demonstrated by the rapid transport of i.v. injected fluorescent tracer (dextran–Texas Red) that highlights the ER-TR7$^+$ reticular network within minutes after injection (Figure 4F). Similar to LNs, major histocompatibility complex class II$^+$ DCs were associated on the outside of the podoplanin$^+$ cells, possibly retrieving antigen from the conduit lumen[13] (Figure 4G). In summary, functional conduits develop in T-cell–rich areas of TLTs and are tightly associated with TRCs, the likely producers of these ECM molecules. Because of the high phenotypic and functional resemblance of TRC-like cells in TLTs with their counterpart in SLOs, we will refer to them as TRCs as well.
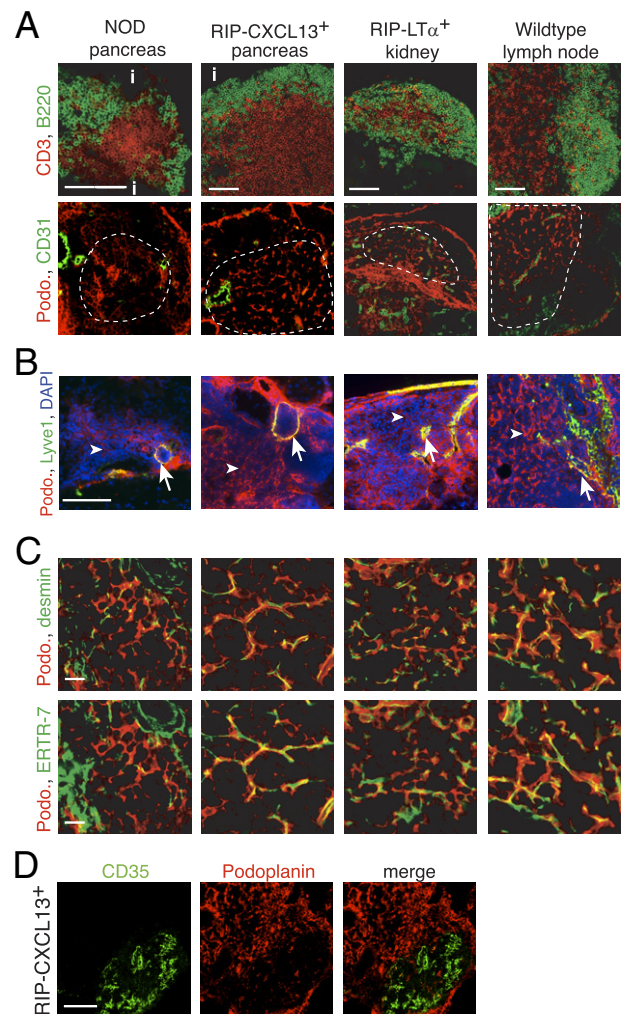
Figure 3. The TLTs developing in murine models of chronic inflammation form a network of podoplanin$^+$ stromal cells in the T zone, similar to LNs. Immunofluorescence analysis of frozen sections of pancreas from NOD and RIP-CXCL13 tg$^+$ mice and kidney from RIP-LTα tg$^+$ mice and peripheral LNs. **A:** B220$^+$ B cells (green) and CD3$^+$ T cells (red), the TRC marker podoplanin (podo, red) combined with the endothelial marker CD31 (green) in serial sections. Tg$^-$ pancreata did not show reticular podoplanin staining typical for TRCs (data not shown). Scale bar = 100 μm. i indicates islet. **B:** Infiltrate labeled with podoplanin (red), the lymphatic vessel marker Lyve-1 (green), and DAPI$^+$ nuclei (blue). **Arrows** indicate lymphatic vessels; and **arrowheads**, the more abundant fibroblastic reticular cells. Scale bar = 100 μm. **C:** Higher-magnification images of the T-cell–rich zone of the infiltrate labeled with podoplanin (red) and desmin and the conduit marker ER-TR7 (green). Scale bar = 20 μm. **D:** The podoplanin (red) and CD35 (green) staining showing two distinct stromal cell networks in infiltrates of RIP-CXCL13$^+$ pancreas. Scale bar = 100 μm. Data are representative of at least three independent experiments.
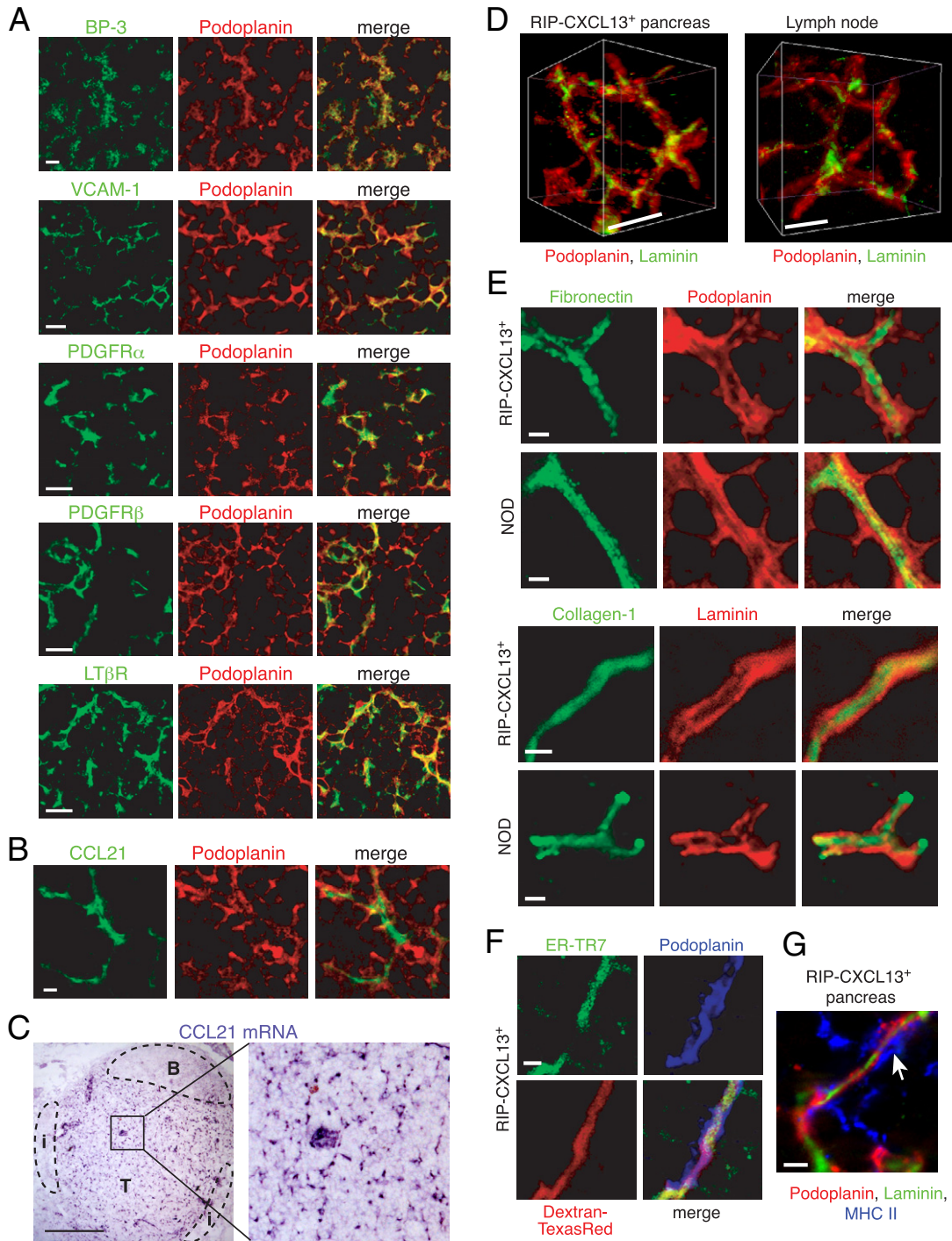
Figure 4. Phenotype of podoplanin^{+} stromal cells and matrix structures in T-cell–rich zones of pancreatic infiltrates in RIP-CXCL13 tg[+] mice. **A:** Confocal immunofluorescence analysis of sections stained with markers for podoplanin (red) and BP-3, VCAM-1, PDGFRα, PDGFRβ, and LTβR (all green). Scale bars = 10 μm. **B:** Immunofluorescence analysis of pancreatic sections of RIP-CXCL13 tg[+] mice labeled with antibodies against CCL21 (green) and podoplanin (red). Scale bar = 2 μm. Data are representative of three independent experiments. **C:** *In situ* hybridization analysis for *Ccl21* transcripts in pancreatic infiltrates of RIP-CXCL13 tg[+] mice. Tg[−] pancreas showed only *Ccl21* transcripts on lymphatic vessels distant from the islets (not shown). Scale bar = 100 μm. B indicates B zone; T, T zone; i, islet. Confocal immunofluorescence images from vibratome (**D** and **G**) or 8-μm-thick sections (**E** and **F**). **D:** The 3D reconstruction of images from T-cell–rich zones of pancreatic infiltrates of RIP-CXCL13 tg[+] mice and of LNs labeled with podoplanin (red) and laminin (green). Scale bars = 5 μm. **E:** T-cell–rich zone in sections from RIP-CXCL13 tg[+] and NOD pancreas labeled with antibodies against the TRC marker podoplanin (red) and the conduit markers fibronectin (green), laminin (red), and collagen-1 (green). Scale bars = 2 μm. **F:** Pancreas sections of RIP-CXCL13 tg[+] mice that were injected i.v. with the tracer dextran–Texas Red 10 minutes before isolating and fixing the tissue. Sections were costained with antibodies against ER-TR7 (green) and podoplanin (blue). Scale bar = 2 μm. **G:** T-cell–rich zone of infiltrates in RIP-CXCL13 tg[+] pancreas labeled with podoplanin (red), laminin (green), and MHC II (blue). Scale bar = 5 μm. Data are representative of at least two independent experiments.

Maintenance of Ectopic TRC Networks and Conduits Is Largely LTαβ Dependent

The formation and maintenance of several lymphoid structures in CXCL13-transgenic pancreata is known to be LTα and LTβR dependent, including HEVs, BP-3^{+}, and CCL21^{+} stromal cells.[21] To determine whether LTβR signaling was also involved in the maintenance of podoplanin[+] TRC networks and conduits in RIP-CXCL13 tg[+] mice, they were treated for 22 days with LTβR-Fc fusion protein, leading to the disappearance of most large infiltrates (see Supplemental Figure S5A at *http://ajp.amjpathol.org*).[21] The remaining infiltrates showed small T-cell–rich zones that correlated with a marked reduction in the extent of the reticular TRC network (podoplanin^{+} CD31^{−}Lyve1^{−}) and of CD31^{+} blood vessels and Lyve1^{+} lymphatic vessels (Figure 5, A and B). Surprisingly, staining with antibodies against podoplanin, fibronectin, laminin, and collagen-1 revealed that the overall structure of the small remaining TRC network and conduits was not altered in LTβR-Fc–treated mice (Figure 5C, see Supplemental Figure S5B at *http://ajp.amjpathol.org*). In some infiltrates, the expression of the chemokine CCL21 was still detectable after LTβR-Fc treatment but always in a much reduced area (Figure 5D), confirming an earlier report[21] and correlating with the smaller podoplanin[+] TRC network. Therefore, the maintenance of functional and well-developed T zones in RIP-CXCL13 tg[+] mice, including TRC networks and their associated conduits, is partially dependent on continuing LTβR signaling.

LTi Cells Are Present in Adult Secondary and TLTs

To test if LTi cells could play a role as the LTαβ source in the formation of TLTs and LTβR[+] TRC networks in particular, we crossed RIP-CXCL13 tg[+] mice to mice deficient in the transcription factor RORγ, which lack LTi cells and, consequently, all LNs and PPs.[41] We confirmed by flow cytometry that few CD4^{+} CD3^{−} CD45^{+} LTi cells expressing IL-7Rα and LTβR ligands can be found in the LNs and spleen of adult wild-type mice (Figure 6A), as previously reported.[35,36,45] Consistent with the RORγ requirement of LTi cell development, cells with this phenotype were completely absent from spleens of adult RORγ^{−/−} mice (Figure 6A), confirming an earlier report[35] on RORγ^{−/−} bone marrow chimeras. The CD4^{+} CD3^{−} cells expressing IL-7Rα and LTβR ligands were also detected in the pancreas of adult RIP-CXCL13–transgenic mice, but not in nontransgenic littermates or transgenic mice on an RORγ-deficient background (Figure 6B, data not shown). In the three mouse strains, we did not obtain strong evidence for CD4^{−} LTi cells because most CD4^{−} CD3^{−} cells were negative for IL-7Rα and LTβR ligands.[46] Strikingly, in RIP-CXCL13–transgenic pancreas, the LTi frequency was in a similar range as in the SLOs of adult mice (Figure 6, A and B). Histological analysis showed that most IL-7Rα^{+} CD3^{−} cells localized to perifollicular regions in the pancreatic infiltrates, similar to adult LNs and spleen (Figure 6C).[45] The phenotype and localization of these cells in adult tissues suggest they are LTi cells. This finding raises the possibility of cross
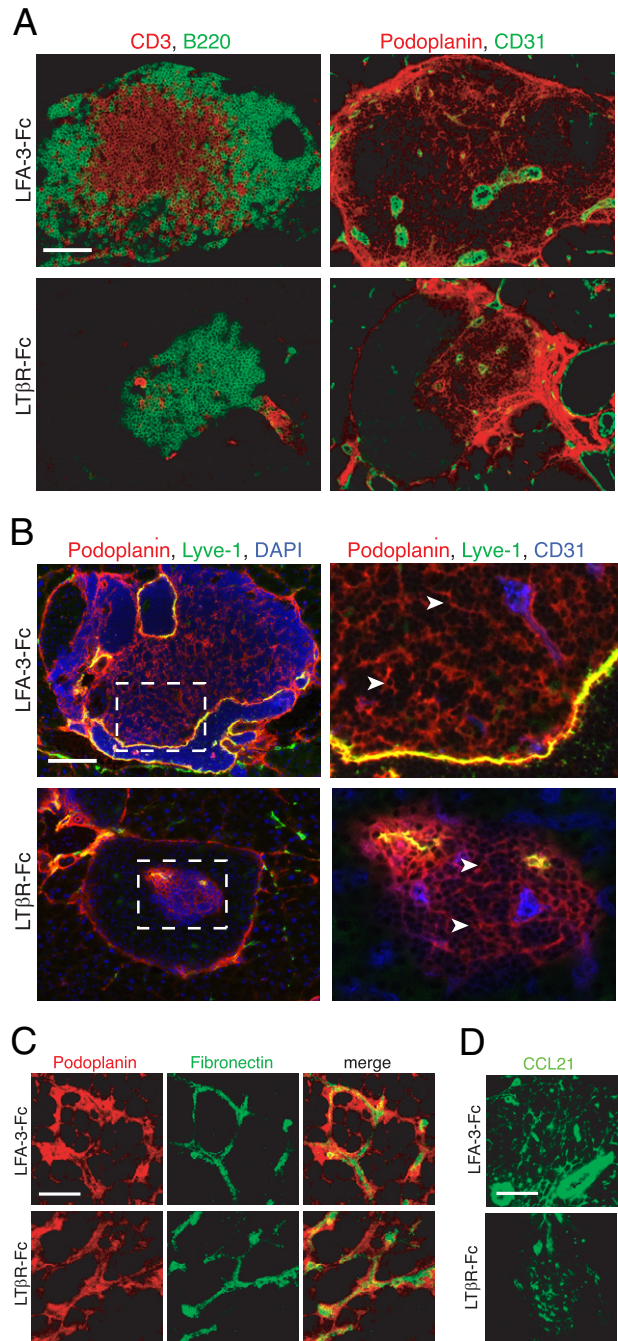
Figure 5. Maintenance of the ectopic TRC network and the conduit system in RIP-CXCL13 tg[+] pancreas is partially LTβR dependent. Immunofluorescence analysis of 8-μm-thick pancreas sections from adult RIP-CXCL13 tg[+] mice (aged 4 months) treated twice per week for 22 days with 100 μg of soluble LTβR-Fc or control LFA-3-Fc fusion proteins. Data are representative of three mice per group. **A:** Serial frozen sections were stained for CD3^{+} T cells (red) and B220^{+} B cells (green) and for podoplanin (red) and CD31 (green). Scale bar = 100 μm. **B:** Staining of an infiltrated islet for podoplanin (red), lyve-1 (green), and DAPI[+] nuclei (blue), with the clustered DAPI^{+} cells representing mainly infiltrating T and B cells. Lymphatic vessels appear in yellow (podoplanin[+]lyve1[+]); and reticular fibroblasts in red (podoplanin[+]lyve1[−]). **Right:** A higher magnification of the infiltrate is shown with the vascular marker CD31 instead of DAPI (blue). Most podoplanin^{+} cells (**arrowheads**) show reticular morphological features and absence of vascular markers (Lyve1^{−}CD31^{−}). **C:** Confocal images showing podoplanin^{+} cells (red) and fibronectin^{+} conduits (green) in the T-cell–rich region. Scale bar = 10 μm. **D:** Immunofluorescence analysis of CCL21 (green) expression in the podoplanin[+] region. Scale bar = 100 μm.
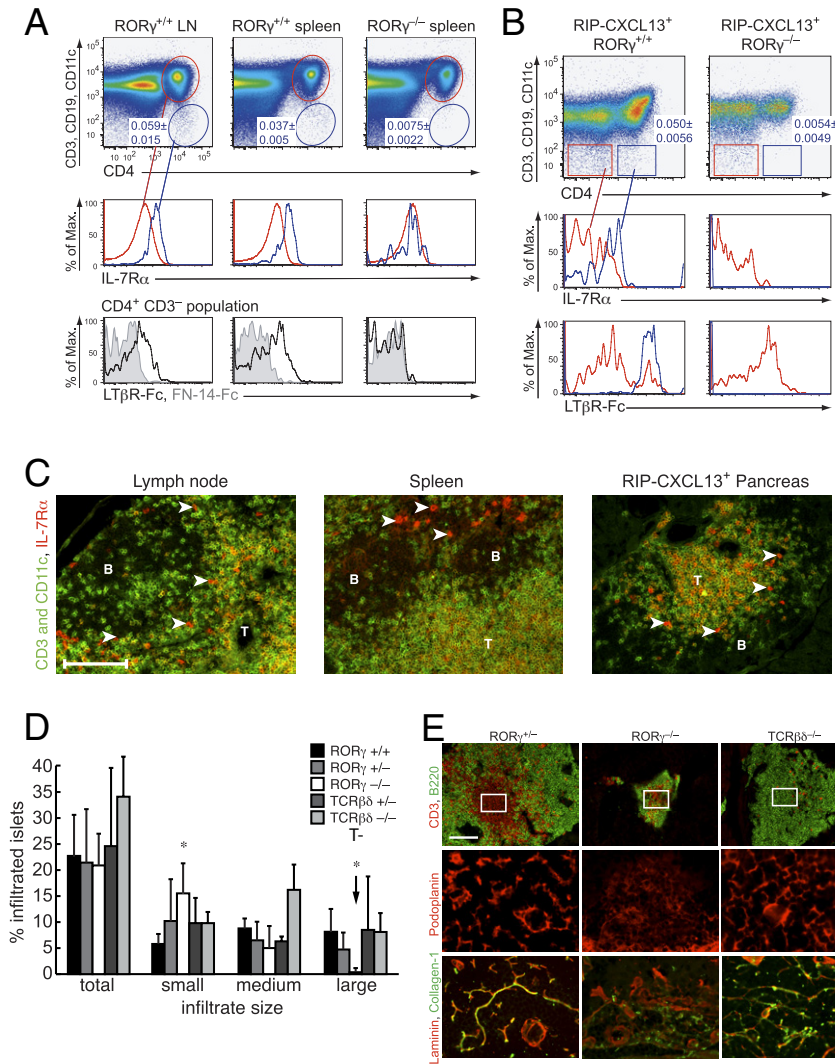
Figure 6. The RORγ-dependent LTi cells are present in adult wild-type spleen and pancreatic infiltrates of adult RIP-CXCL13 tg+ mice and are critical for the development of larger pancreatic infiltrates with TRC networks and conduit systems. **A:** Flow cytometric analysis of single-cell suspensions prepared from adult peripheral LNs and the spleen of RORγ+/+ and RORγ−/− mice. Dot blots are pregated for CD45+ cells. Gates indicate CD4+ CD3+ (T cells; red) and CD4+ CD3− CD11c− CD19− (LTi like; blue) populations (n = 3). Histograms show IL-7Rα expression on these two populations and LTβR ligand expression on the CD4+ CD3− LTi cell population, detected with LTβR-Fc compared with the control FN14-Fc fusion protein. **B:** Hematopoietic cells were isolated from the pancreas of adult RIP-CXCL13 tg+ mice on an RORγ+/+ or RORγ−/− background. Dot blots are pregated for CD45+ cells and show CD4+ CD3− CD11c− CD19− (LTi-like; blue) and CD4− CD3− CD11c− CD19− (red) populations (n = 3). Histograms show IL-7Rα and LTβR ligand expression on these two populations. **C:** Serial frozen sections of peripheral LNs, spleen, and pancreas of RIP-CXCL13 tg+ mice were stained with antibodies to IL-7Rα (red) and CD3/CD11c (green). **Arrowheads** indicate IL-7Rα+ CD3− CD11c− LTi-like cells in perifollicular regions. Scale bar = 100 μm. **A** through **C:** Data are representative of at least three independent experiments. B, B cell-rich zone; T, T cell rich zone. **D:** Pancreata from RIP-CXCL13 tg+ mice crossed onto the RORγ−/− and TCRβδ−/− background were sectioned (10 μm), and every 15th section was stained with hematoxylin and analyzed for the frequency and size of islet-associated mononuclear infiltrates. Results were derived from 100 to 200 islets in each of the three transgenic mice per group (littermates aged 7 to 12 weeks).[21] The frequencies of small (5 to 30 hematopoietic cells/infiltrate in a section), medium (31 to 300 cells), and large (greater than 300 cells) infiltrates and total infiltrates are shown. **Arrow** indicates the striking reduction of large infiltrates in tg+ mice on a RORγ−/− background. **E:** Sections of RIP-CXCL13 tg+ pancreata on an RORγ+/−, RORγ−/−, or TCRβδ−/− background were labeled for CD3+ T cells (red) and B220+ B cells (green). Examples of the largest infiltrates in each mouse are shown. Scale bar = 100 μm. The white squares indicate the area chosen in the consecutive sections to show staining for podoplanin+ cells (red) and laminin+ (red) and collagen-1+ (green) conduits.

talk between these LTi cells and LTβR+ TRCs found in the same zone.

Formation of Large Infiltrates in RIP-CXCL13– Transgenic Mice Is Dependent On RORγ But Not T Cells

To test whether LTi cells play a role in the formation and maintenance of TLTs, we performed a histological analysis of pancreatic infiltrates in RORγ-deficient RIP-CXCL13 tg+ mice. Hematoxylin-stained sections revealed a striking deficiency in the formation of large infiltrates in these mice (Figure 6D). Only large infiltrates (more than 300 cells) have previously displayed clearly defined T- and B-cell–rich zones, along with extensive BP-3 and CCL21 expression.[21] Therefore, we analyzed the composition and organization of infiltrates in RORγ-deficient RIP-CXCL13 mice using immunofluorescence microscopy. The small and few medium-sized infiltrates in these mice consisted of B cells and a few T cells that were not well segregated (Figure 6E). Distinct

podoplanin+ TRC networks were lacking within the infiltrates while they were present within the spleen (data not shown). Podoplanin was only detected on the islet capsule and lymphatic vessels, similar to wild-type pancreata. The TRC-associated conduits were mostly absent, based on stainings for fibronectin, collagen I, laminin, ER-TR7, and CCL21 (Figure 6E, see Supplemental Figure S6 at *http://ajp. amjpathol.org*). Interestingly, PNAd- and MAdCAM1-positive HEVs were also strongly reduced in the infiltrates (see Supplemental Figure S6 at *http://ajp.amjpathol.org*). To exclude that the failure to develop TLTs in RORγ−/− mice was because of altered expression of LTαβ on B cells, we compared wild-type with RORγ−/− B cells by flow cytometric analysis. Yet, no difference in LTβR-Fc staining could be detected (see Supplemental Figure S7 at *http://ajp.amjpathol. org*). In addition to lacking LTi cells, RORγ−/− mice have strongly reduced numbers of mature T cells[41] and lack type 17 helper T cell and natural killer p46+ cell subsets.[47] To exclude a role for T cells in TLT formation, TCRβδ-deficient RIP-CXCL13 tg+ mice were analyzed. These mice showed

normal development of large infiltrates containing mainly B cells. Interestingly, extensive podoplanin[+] cell networks and fibronectin[+] conduits developed in central parts of the B-cell–dominated infiltrates (Figure 6E, data not shown). In addition, PNAd[+] and MAdCAM[+] HEVs also developed normally (see Supplemental Figure S6 at *http://ajp.amjpathol. org*). These data indicate that the presence of LTi and/or possibly natural killer p46[+], but not T cells, is required for the development of large LN-like structures in adult RIP-CXCL13 pancreas, including TRC networks, conduits, and HEVs.

Discussion

Stromal cells may play a key role in the switch leading from acute resolving to chronic persistent inflammation.[1] Therefore, we performed a comprehensive analysis of reticular stromal cells arising in various types of TLTs in human disease and murine models of inflammation in which TLTs form. We found that the T-cell–rich region of TLTs contains a TRC-like stromal cell type similar to LNs. It is distinct from FDCs in B zones. Therefore, larger TLTs closely replicate the stromal cell organization of SLOs that is critical for T- and B-zone compartmentalization.

In TLTs of NOD, RIP-LTα, and RIP-CXCL13 transgenic mice, extensive T-zone stromal cell networks were identified based on the following surface phenotype: podoplanin^{+} CD31^{−} CD35^{−}. These cells also expressed other TRC markers, including LTβR and its potential downstream targets (ie, BP-3 and VCAM-1).[10,12] The coexpression of PDGFRα, PDGFRβ, and desmin is consistent with a mesenchymal origin for these cells and suggests that they may be functional myofibroblasts similar to their counterparts in LNs and wound healing.[10] In support of this notion, we observed low αSMA expression in these cells (data not shown). The cell morphological features were characterized by long and fine processes typical for fibroblastic reticular cells and distinct from endothelial vessels. They wrapped around ECM structures comparable in composition and organization to the conduits in SLOs,[7,12–14] extending previous studies[20,23–25,48,49] showing reticulin and ER-TR7 staining in TLTs. We demonstrate herein that these conduits contain CCL21 and are functional because they can transport small-molecular-weight molecules. The elucidation of their precise function for TLT function will need further work. Thus far, functional conduits had only been described for LNs, spleen, and thymus.[14,50,51] Similar to the two latter organs, it seems plausible that conduits in TLTs start next to blood vessels and drain the exudate, including blood-borne molecules and blood serum. In conclusion, the phenotype, organization, and compartmentalization of TRC-like cells, found in larger murine TLTs, are indistinguishable from their counterparts in SLOs.

One of the key functions of TRCs in SLOs is the secretion of CCL19 and CCL21.[9,10] During the past few years, expression levels of CCL19 and CCL21 have been reported for various murine TLTs[2,3,49] and occasionally in tumors.[22,52] The CCL21 protein staining in murine TLTs was associated with HEVs and lymphatic vessels.[2,3] Reticular

CCL21 protein staining was previously reported in RIP-CXCL13 tg[+] infiltrates.[21] Herein, we show that most reticular CCL21 protein staining localizes to the conduits, suggesting active chemokine transport. Because CCL21 transcripts are also found in a reticular pattern throughout the T zone, it is likely that the podoplanin^{+} stromal cells forming a 3D network are the major local CCL21 source mediating the attraction of CCR7^{+} T cells and DCs. Indeed, DCs, presumably CCR7^{+}, were often observed immediately adjacent to the podoplanin^{+} cells, suggesting active adhesion of DCs to this network, similar to LNs.[8,53] T cells localized within the TRC network, suggesting that TRC-derived CCL21 promotes T-cell attraction and local motility that is thought to be critical for efficient selection of the rare antigen-specific T cells in SLOs.[54] Therefore, we propose that TRC-like cells in TLTs reproduce both the structure and function of T zones in SLOs. They form a functional scaffold that brings together T cells with antigen-bearing DCs, thereby driving the local adaptive immune response, in addition to its potential role in angiogenesis of blood and lymphatic vessels. This notion is supported by a recent molecular analysis[22] of TRCs from LNs and sites of inflammation and tumors, where TRCs were a source of transcripts for IL-7 and CCL19/21 and of angiogenic factors.

The second reticular stromal cell type present in SLOs, FDCs, has been previously described in many types of murine TLTs using CD35 and FDC-M1 as FDC-specific markers.[2,3] In RIP-CXCL13 tg^{+} mice, only large infiltrates contained CD35^{+} FDC networks that localized among B-cell–rich areas and were not in contact with T cells, DCs, and HEVs. They were podoplanin^{low} and PDGFRα/β[−] and did not associate with CCL21 protein and conduits. Therefore, FDCs and TRCs found in TLTs are two separate reticular cell types with distinct anatomical localization (B- or T-cell zones) and function. In addition to providing structural support, we propose that these two networks and their chemokine expression profiles provide the underlying organizing principle of B- and T-zone segregation observed in many pathological TLTs,[2,3] similar to their physiological counterparts in SLOs.[55] How they develop and influence the local regulation of immune responses during disease remains to be shown.

Although FDCs have been well characterized in human SLOs and TLTs, little is known about the stromal cells of the T zone.[2,3] Their presence in SLOs was described in several morphological studies[56,57] showing a reticular network in T zones. Recently, a network of αSMA^{+} cells colocalizing with CCL19 and CCL21 expression was conserved in the SLOs and TLTs of patients with rheumatoid arthritis.[26] Herein, we extend these findings by showing that these cells in SLOs and TLTs resemble each other, based on their surface phenotype (podoplanin^{+} CD21^{−}) and function (ECM production and conduits). Podoplanin^{+} CD21^{−} TRCs had long cell processes, formed a 3D reticular network, localized to T-cell–rich zones, and associated with complex ECM structures resembling conduits and with CCL21 protein and CD11c^{+} DCs. When cultured *in vitro*, these podoplanin^{+} cells exhibited typical fibroblast morphological features and showed high expression of ECM molecules and variable levels of αSMA (our unpublished data), similar to their murine counterparts[12] (our unpublished data). Within the same

TLT, we observed heterogeneity in the amount of CCL21 and ECM associated with the TRCs that could indicate different degrees of TRC differentiation or activation. The ECM staining, similar to that observed in LN T zones, has previously been described in the samples of patients with multiple sclerosis, suggesting that conduits and possibly TRC-like cells may be present in many more sites of chronic inflammation.[58] In summary, TRC-like cells are a frequent component of ectopic infiltrates associated with human disease and closely resemble their SLO counterparts. They are likely to contribute, together with FDCs, to the overall organization and possible pathogenic function of human TLTs.

Given the frequent presence of TRCs at sites of chronic inflammation, understanding their development becomes an important issue. In this study, we show that the maintenance of the complex TRC network with its conduit structures within infiltrates of RIP-CXCL13 transgenic mice is partially dependent on LTβR signals, reminiscent of previous observations with HEVs.[21,33] Other unidentified receptors appear to contribute to the formation of small and medium-sized infiltrates containing small TRC networks, with possible candidates being tumor necrosis factor-R1 and CD30.[12,59] We propose that LTβR signals may be critical for the development and/or maintenance of larger and more differentiated stromal cell compartments, as observed in large infiltrates. The LTβR signaling can be triggered by two ligands (ie, LT$\alpha\beta$ and LIGHT).[33,60] Because the formation of pancreatic infiltrates in RIP-CXCL13 transgenic mice was largely dependent on LTα[21] and the effects of LIGHT deficiency on lymphoid organ development are minor compared with LT$\alpha\beta$,[60] we suggest that LT$\alpha\beta$ is likely to be the dominant LTβR ligand for TLT formation. Signaling via LTβR on stromal cells is thought to be the key pathway inducing the expression of CCL19 and CCL21 in TRCs and of CXCL13 in FDCs. Because these chemokines, in turn, attract lymphocytes and further induce their LT$\alpha\beta$ expression,[55,60] this stromal-hematopoietic cross talk may lead to a positive feedback loop, allowing the further growth and organization of infiltrates, analogous to the process of embryonic LN/PP development. Blocking of LTβR signaling in RIP-CXCL13 tg$^+$ mice likely interrupts this feedback loop and leads to a decreased size of the TRC network and conduit system. Although this may contribute to the reduction in TLT cellularity, the disappearance of well-differentiated HEVs, expressing integrin ligands, is likely to play an important role as well.[33] In contrast to LNs, neutralization of LTβR signaling in adult mice partially disrupts stromal cell networks in splenic T and B zones, including CCL21 and CXCL13 expression.[33,55] Therefore, stromal cells in TLTs resemble those in spleen because both depend on a continuous dialogue with LT$\alpha\beta^+$ hematopoietic cells. In several other inflammatory models, such as RIP-CCL21 tg$^+$, NOD, experimental autoimmune encephalitis, apolipoprotein E$^{-/-}$, and influenza-infected mice, blocking LTβR leads to a strong reduction of TLT size and organization.[33,49,61] Because the associated pathological features were reduced by this treatment, this pathway holds promise as a future drug target.[33,62]

The LTα1β2 signal required for splenic white pulp development is given by B cells and possibly LTi cells, whereas LTi cells are sufficient to provide this signal during early LN and PP development.[27,28,34,63] Several recent studies have suggested that CD4$^+$ CD3$^-$ LTi cells can persist into adulthood. Within the adult spleen, LTi-like cells may have organized T cell B cell segregation,[34] repaired damaged stromal cell networks,[35] and improved memory formation.[45] Preliminary evidence[37,38,64] suggested a role for LTi cells in CXCL13- or IL-7–induced TLT formation. We detected a population of CD4$^+$ CD3$^-$ cells expressing IL-7Rα and LT$\alpha\beta$ in the spleen and LNs of adult mice and within pancreatic infiltrates of adult RIP-CXCL13 tg$^+$ mice. They share this phenotype with neonatal LTi cells and were absent from the spleen and pancreas of RORγ-deficient mice. Surprisingly, the absence of LTi cells reduced the size and organization of the infiltrate to a similar extent as the lack of LTα.[21] The absence of B cells led to even smaller infiltrates, possibly because B cells are the main cell population attracted by CXCL13.[21] The other possibility is that both LTi and B cells provide LT$\alpha\beta$ signals to stromal cell precursors, possibly in a sequential manner. The appearance of LTi cells in RIP-CXCL13$^+$ pancreata before birth was reported, with B cells colonizing shortly thereafter.[37] Distinct lymphocyte accumulations become visible only 1 to 3 weeks after birth (our unpublished data), indicating that they develop postnatally, along with nasal-associated lymphoid tissue and PPs; therefore, they may be considered ectopic LNs. Because both cell types are still present in the infiltrates of adult mice, both may contribute to LT$\alpha\beta$-dependent TLT maintenance. The colocalization of LT$\alpha\beta^+$ LTi cells with LTβR$^+$ TRCs would be consistent with such an interaction that may lead to chemokine expression, as reported in other systems.[34,35]

The CD4$^+$ CD3$^-$ cells were also detected in ectopic lymphoid infiltrates of adult *apolipoprotein E*$^{-/-}$[65] and villin-CXCL13 transgenic mice[64]; they could play a similar role in these mice. Ectopic LNs and PPs, developing in IL-7–overexpressing mice, were RORγ and LTα dependent, implying LTi cell involvement.[38] In contrast, the lack of LTi cells [due to deficiency of inhibitor of DNA-binding (Id) 2] or LTα did not influence the formation of TLTs in a model in which CCL21 expression was expressed in the thyroid.[25] This discrepancy may stem from the potential heterogeneity among LTi cells, with some being RORγ and others being Id2 dependent.[4] Alternatively, the onset of tissue infiltration may differ, with lymphocytes infiltrating early after birth in RIP-CXCL13$^+$ pancreata and possibly later in CCL21-overexpressing thyroid. Interestingly, RIP-CCL21 tg$^+$ pancreata also contain LTi cells shortly after birth (our unpublished data), suggesting that both CXCL13 and CCL21 can attract LTi cells. Yet another difference may be the cell type providing lymphoid tissue–inducing signals (LT$\alpha\beta$ or other) because B, T, or natural killer cells could replace LTi cells in their inductive function, especially when they are activated.[60] In many autoimmune diseases, sufficient LT$\alpha\beta$ is likely provided by activated lymphocytes.[4] In line with this notion, we have not been able to reproducibly detect LTi cells in NOD pancreas (data not shown), possibly because of the relatively low expression of LTi attractants, such as CXCL13 and CCL21, at the inflammatory site.[20] More studies[4] using different murine TLT models are required to clarify whether LTi cells are a frequent feature of the development of ectopic lymphoid structures. Similar studies[47]

should be performed on human tissues because human LTi-like cells have also been recently described. Given that podoplanin[+] TRC can evolve at sites of acute inflammation in the absence of LT$\alpha\beta$ signals, the pathways leading to TRC formation are likely to be redundant, thereby increasing the robustness of the system.[22]

In summary, we demonstrate that the similarities between SLOs and ectopic lymphoid tissues (TLTs) extend further than previously appreciated. Lymphocytes, FDCs, and HEVs are characteristic features, as are the TRC network and the conduit system. The markers used in this study to identify TRCs should facilitate further examination of these cells in inflammatory diseases, both in mice and humans. In particular, podoplanin as a surface marker will allow isolation of these cells *ex vivo* and investigation of them further, both phenotypically and functionally. Finally, because TRCs are the main producers of the chemokines (ie, CCL19 and CCL21), TRCs might play an important role in the perpetuation of chronic inflammation and could represent an interesting target for therapy.

Acknowledgments

References

1. Buckley CD, Pilling D, Lord JM, Akbar AN, Scheel-Toellner D, Salmon M: Fibroblasts regulate the switch from acute resolving to chronic persistent inflammation. Trends Immunol 2001, 22:199–204
2. Aloisi F, Pujol-Borrell R: Lymphoid neogenesis in chronic inflammatory diseases. Nat Rev Immunol 2006, 6:205–217
3. Drayton DL, Liao S, Mounzer RH, Ruddle NH: Lymphoid organ development: from ontogeny to neogenesis. Nat Immunol 2006, 7:344–353
4. Carragher DM, Rangel-Moreno J, Randall TD: Ectopic lymphoid tissues and local immunity. Semin Immunol 2008, 20:26–42
5. Allen CD, Cyster JG: Follicular dendritic cell networks of primary follicles and germinal centers: phenotype and function. Semin Immunol 2008, 20:14–25
6. Farr AG, Berry ML, Kim A, Nelson AJ, Welch MP, Aruffo A: Characterization and cloning of a novel glycoprotein expressed by stromal cells in T-dependent areas of peripheral lymphoid tissues. J Exp Med 1992, 176:1477–1482
7. Gretz JE, Anderson AO, Shaw S: Cords, channels, corridors and conduits: critical architectural elements facilitating cell interactions in the lymph node cortex. Immunol Rev 1997, 156:11–24
8. Bajenoff M, Egen JG, Koo LY, Laugier JP, Brau F, Glaichenhaus N, Germain RN: Stromal cell networks regulate lymphocyte entry, migration, and territoriality in lymph nodes. Immunity 2006, 25:989–1001
9. Luther SA, Tang HL, Hyman PL, Farr AG, Cyster JG: Coexpression of the chemokines ELC and SLC by T zone stromal cells and deletion of the ELC gene in the plt/plt mouse. Proc Natl Acad Sci U S A 2000, 97:12694–12699
10. Link A, Vogt TK, Favre S, Britschgi MR, Acha-Orbea H, Hinz B, Cyster JG, Luther SA: Fibroblastic reticular cells in lymph nodes regulate the homeostasis of naive T cells. Nat Immunol 2007, 8:1255–1265
11. Forster R, Pabst O, Bernhardt G: Homeostatic chemokines in development, plasticity, and functional organization of the intestinal immune system. Semin Immunol 2008, 20:171–180

12. Katakai T, Hara T, Sugai M, Gonda H, Shimizu A: Lymph node fibroblastic reticular cells construct the stromal reticulum via contact with lymphocytes. J Exp Med 2004, 200:783–795
13. Sixt M, Kanazawa N, Selg M, Samson T, Roos G, Reinhardt DP, Pabst R, Lutz MB, Sorokin L: The conduit system transports soluble antigens from the afferent lymph to resident dendritic cells in the T cell area of the lymph node. Immunity 2005, 22:19–29
14. Gretz JE, Norbury CC, Anderson AO, Proudfoot AE, Shaw S: Lymph-borne chemokines and other low molecular weight molecules reach high endothelial venules via specialized conduits while a functional barrier limits access to the lymphocyte microenvironments in lymph node cortex. J Exp Med 2000, 192:1425–1440
15. Breiteneder-Geleff S, Soleiman A, Kowalski H, Horvat R, Amann G, Kriehuber E, Diem K, Weninger W, Tschachler E, Alitalo K, Kerjaschki D: Angiosarcomas express mixed endothelial phenotypes of blood and lymphatic capillaries: podoplanin as a specific marker for lymphatic endothelium. Am J Pathol 1999, 154:385–394
16. Marsee DK, Pinkus GS, Hornick JL: Podoplanin (D2-40) is a highly effective marker of follicular dendritic cells. Appl Immunohistochem Mol Morphol 2009, 17:102–107
17. Xie Q, Chen L, Fu K, Harter J, Young KH, Sunkara J, Novak D, Villanueva-Siles E, Ratech H: Podoplanin (d2-40): a new immunohistochemical marker for reactive follicular dendritic cells and follicular dendritic cell sarcomas. Int J Clin Exp Pathol 2008, 1:276–284
18. Kawase A, Ishii G, Nagai K, Ito T, Nagano T, Murata Y, Hishida T, Nishimura M, Yoshida J, Suzuki K, Ochiai A: Podoplanin expression by cancer associated fibroblasts predicts poor prognosis of lung adenocarcinoma. Int J Cancer 2008, 123:1053–1059
19. Yamanashi T, Nakanishi Y, Fujii G, Akishima-Fukasawa Y, Moriya Y, Kanai Y, Watanabe M, Hirohashi S: Podoplanin expression identified in stromal fibroblasts as a favorable prognostic marker in patients with colorectal carcinoma. Oncology 2009, 77:53–62
20. Luther SA, Bidgol A, Hargreaves DC, Schmidt A, Xu Y, Paniyadi J, Matloubian M, Cyster JG: Differing activities of homeostatic chemokines CCL19, CCL21, and CXCL12 in lymphocyte and dendritic cell recruitment and lymphoid neogenesis. J Immunol 2002, 169:424–433
21. Luther SA, Lopez T, Bai W, Hanahan D, Cyster JG: BLC expression in pancreatic islets causes B cell recruitment and lymphotoxin-dependent lymphoid neogenesis. Immunity 2000, 12:471–481
22. Peduto L, Dulauroy S, Lochner M, Spath GF, Morales MA, Cumano A, Eberl G: Inflammation recapitulates the ontogeny of lymphoid stromal cells. J Immunol 2009, 182:5789–5799
23. Fan L, Reilly CR, Luo Y, Dorf ME, Lo D: Cutting edge: ectopic expression of the chemokine TCA4/SLC is sufficient to trigger lymphoid neogenesis. J Immunol 2000, 164:3955–3959
24. Katakai T, Hara T, Sugai M, Gonda H, Shimizu A: Th1-biased tertiary lymphoid tissue supported by CXC chemokine ligand 13-producing stromal network in chronic lesions of autoimmune gastritis. J Immunol 2003, 171:4359–4368
25. Marinkovic T, Garin A, Yokota Y, Fu YX, Ruddle NH, Furtado GC, Lira SA: Interaction of mature CD3+CD4+ T cells with dendritic cells triggers the development of tertiary lymphoid structures in the thyroid. J Clin Invest 2006, 116:2622–2632
26. Manzo A, Bugatti S, Caporali R, Prevo R, Jackson DG, Uguccioni M, Buckley CD, Montecucco C, Pitzalis C: CCL21 expression pattern of human secondary lymphoid organ stroma is conserved in inflammatory lesions with lymphoid neogenesis. Am J Pathol 2007, 171:1549–1562
27. Honda K, Nakano H, Yoshida H, Nishikawa S, Rennert P, Ikuta K, Tamechika M, Yamaguchi K, Fukumoto T, Chiba T, Nishikawa SI: Molecular basis for hematopoietic/mesenchymal interaction during initiation of Peyer's patch organogenesis. J Exp Med 2001, 193:621–630
28. Cupedo T, Mebius RE: Cellular interactions in lymph node development. J Immunol 2005, 174:21–25
29. Picarella DE, Kratz A, Li CB, Ruddle NH, Flavell RA: Insulitis in transgenic mice expressing tumor necrosis factor beta (lymphotoxin) in the pancreas. Proc Natl Acad Sci U S A 1992, 89:10036–10040
30. Kratz A, Campos-Neto A, Hanson MS, Ruddle NH: Chronic inflammation caused by lymphotoxin is lymphoid neogenesis. J Exp Med 1996, 183:1461–1472
31. Chen SC, Vassileva G, Kinsley D, Holzmann S, Manfra D, Wiekowski MT, Romani N, Lira SA: Ectopic expression of the murine chemokines CCL21a and CCL21b induces the formation of lymph node-like struc-

tures in pancreas, but not skin, of transgenic mice. J Immunol 2002, 168:1001–1008

32. Martin AP, Canasto-Chibuque C, Shang L, Rollins BJ, Lira SA: The chemokine decoy receptor M3 blocks CC chemokine ligand 2 and CXC chemokine ligand 13 function in vivo. J Immunol 2006, 177:7296–7302

33. Browning JL: Inhibition of the lymphotoxin pathway as a therapy for autoimmune disease. Immunol Rev 2008, 223:202–220

34. Kim MY, McConnell FM, Gaspal FM, White A, Glanville SH, Bekiaris V, Walker LS, Caamano J, Jenkinson E, Anderson G, Lane PJ: Function of CD4+CD3- cells in relation to B- and T-zone stroma in spleen. Blood 2007, 109:1602–1610

35. Scandella E, Bolinger B, Lattmann E, Miller S, Favre S, Littman DR, Finke D, Luther SA, Junt T, Ludewig B: Restoration of lymphoid organ integrity through the interaction of lymphoid tissue-inducer cells with stroma of the T cell zone. Nat Immunol 2008, 9:667–675

36. Schmutz S, Bosco N, Chappaz S, Boyman O, Acha-Orbea H, Ceredig R, Rolink AG, Finke D: Cutting edge: IL-7 regulates the peripheral pool of adult ROR gamma+ lymphoid tissue inducer cells. J Immunol 2009, 183:2217–2221

37. Luther SA, Ansel KM, Cyster JG: Overlapping roles of CXCL13, interleukin 7 receptor alpha, and CCR7 ligands in lymph node development. J Exp Med 2003, 197:1191–1198

38. Meier D, Bornmann C, Chappaz S, Schmutz S, Otten LA, Ceredig R, Acha-Orbea H, Finke D: Ectopic lymphoid-organ development occurs through interleukin 7-mediated enhanced survival of lymphoid-tissue-inducer cells. Immunity 2007, 26:643–654

39. Gershwin ME, Mackay IR: The causes of primary biliary cirrhosis: convenient and inconvenient truths. Hepatology 2008, 47:737–745

40. Hansen A, Lipsky PE, Dorner T: Immunopathogenesis of primary Sjogren's syndrome: implications for disease management and therapy. Curr Opin Rheumatol 2005, 17:558–565

41. Sun Z, Unutmaz D, Zou YR, Sunshine MJ, Pierani A, Brenner-Morton S, Mebius RE, Littman DR: Requirement for RORgamma in thymocyte survival and lymphoid organ development. Science 2000, 288:2369–2373

42. Mackay F, Browning JL: Turning off follicular dendritic cells. Nature 1998, 395:26–27

43. Burman A, Haworth O, Hardie DL, Amft EN, Siewert C, Jackson DG, Salmon M, Buckley CD: A chemokine-dependent stromal induction mechanism for aberrant lymphocyte accumulation and compromised lymphatic return in rheumatoid arthritis. J Immunol 2005, 174:1693–1700

44. Anderson MS, Bluestone JA: The NOD mouse: a model of immune dysregulation. Annu Rev Immunol 2005, 23:447–485

45. Kim MY, Gaspal FM, Wiggett HE, McConnell FM, Gulbranson-Judge A, Raykundalia C, Walker LS, Goodall MD, Lane PJ: CD4(+)CD3(−) accessory cells costimulate primed CD4 T cells through OX40 and CD30 at sites where T cells collaborate with B cells. Immunity 2003, 18:643–654

46. Kim MY, Rossi S, Withers D, McConnell F, Toellner KM, Gaspal F, Jenkinson E, Anderson G, Lane PJ: Heterogeneity of lymphoid tissue inducer cell populations present in embryonic and adult mouse lymphoid tissues. Immunology 2008, 124:166–174

47. Vivier E, Spits H, Cupedo T: Interleukin-22-producing innate immune cells: new players in mucosal immunity and tissue repair? Nat Rev Immunol 2009, 9:229–234

48. Higuchi Y, Herrera P, Muniesa P, Huarte J, Belin D, Ohashi P, Aichele P, Orci L, Vassalli JD, Vassalli P: Expression of a tumor necrosis factor alpha transgene in murine pancreatic beta cells results in severe and permanent insulitis without evolution towards diabetes. J Exp Med 1992, 176:1719–1731

49. Grabner R, Lotzer K, Dopping S, Hildner M, Radke D, Beer M, Spanbroek R, Lippert B, Reardon CA, Getz GS, Fu YX, Hehlgans T,

50. Nolte MA, Belien JA, Schadee-Eestermans I, Jansen W, Unger WW, van Rooijen N, Kraal G, Mebius RE: A conduit system distributes chemokines and small blood-borne molecules through the splenic white pulp. J Exp Med 2003, 198:505–512

51. Drumea-Mirancea M, Wessels JT, Muller CA, Essl M, Eble JA, Tolosa E, Koch M, Reinhardt DP, Sixt M, Sorokin L, Stierhof YD, Schwarz H, Klein G: Characterization of a conduit system containing laminin-5 in the human thymus: a potential transport system for small molecules. J Cell Sci 2006, 119:1396–1405

52. Shields JD, Kourtis IC, Tomei AA, Roberts JM, Swartz MA: Induction of lymphoidlike stroma and immune escape by tumors that express the chemokine CCL21. Science 2010, 328:749–752

53. Katakai T, Hara T, Lee JH, Gonda H, Sugai M, Shimizu A: A novel reticular stromal structure in lymph node cortex: an immuno-platform for interactions among dendritic cells: T cells and B cells. Int Immunol 2004, 16:1133–1142

54. Bajenoff M, Egen JG, Qi H, Huang AY, Castellino F, Germain RN: Highways, byways and breadcrumbs: directing lymphocyte traffic in the lymph node. Trends Immunol 2007, 28:346–352

55. Cyster JG: Chemokines, sphingosine-1-phosphate, and cell migration in secondary lymphoid organs. Annu Rev Immunol 2005, 23:127–159

56. Satoh T, Takeda R, Oikawa H, Satodate R: Immunohistochemical and structural characteristics of the reticular framework of the white pulp and marginal zone in the human spleen. Anat Rec 1997, 249:486–494

57. Thomazy VA, Vega F, Medeiros LJ, Davies PJ, Jones D: Phenotypic modulation of the stromal reticular network in normal and neoplastic lymph nodes: tissue transglutaminase reveals coordinate regulation of multiple cell types. Am J Pathol 2003, 163:165–174

58. van Horssen J, Bo L, Dijkstra CD, de Vries HE: Extensive extracellular matrix depositions in active multiple sclerosis lesions. Neurobiol Dis 2006, 24:484–491

59. Bekiaris V, Gaspal F, Kim MY, Withers DR, McConnell FM, Anderson G, Lane PJ: CD30 is required for CCL21 expression and CD4 T cell recruitment in the absence of lymphotoxin signals. J Immunol 2009, 182:4771–4775

60. Schneider K, Potter KG, Ware CF: Lymphotoxin and LIGHT signaling pathways and target genes. Immunol Rev 2004, 202:49–66

61. GeurtsvanKessel CH, Willart MA, Bergen IM, van Rijt LS, Muskens F, Elewaut D, Osterhaus AD, Hendriks R, Rimmelzwaan GF, Lambrecht BN: Dendritic cells are crucial for maintenance of tertiary lymphoid structures in the lung of influenza virus-infected mice. J Exp Med 2009, 206:2339–2349

62. Flavell SJ, Hou TZ, Lax S, Filer AD, Salmon M, Buckley CD: Fibroblasts as novel therapeutic targets in chronic inflammation. Br J Pharmacol 2008, 153(Suppl 1):S241–S246

63. Ngo VN, Cornall RJ, Cyster JG: Splenic T zone development is B cell dependent. J Exp Med 2001, 194:1649–1660

64. Marchesi F, Martin AP, Thirunarayanan N, Devany E, Mayer L, Grisotto MG, Furtado GC, Lira SA: CXCL13 expression in the gut promotes accumulation of IL-22-producing lymphoid tissue-inducer cells, and formation of isolated lymphoid follicles. Mucosal Immunol 2009, 2:486–494

65. Moos MP, John N, Grabner R, Nossmann S, Gunther B, Vollandt R, Funk CD, Kaiser B, Habenicht AJ: The lamina adventitia is the major site of immune cell accumulation in standard chow-fed apolipoprotein E-deficient mice. Arterioscler Thromb Vasc Biol 2005, 25:2386 2391